

# Kinetic steps for the hydrolysis of sphingomyelin by *Bacillus cereus* sphingomyelinase in lipid monolayers

María Laura Fanani and Bruno Maggio<sup>1</sup>

Departamento de Química Biológica-CIQUIBIC, Facultad de Ciencias Químicas, Universidad Nacional de Córdoba, Ciudad Universitaria, 5000 Córdoba, Argentina

**Abstract** The sphingomyelinase (Sphmase) activity degrading sphingomyelin (Sphm) monolayers shows a slow-reaction latency period before exhibiting constant rate catalysis. These two kinetic regions are regulated independently by the lateral surface pressure and by lipids that are biomodulators of cell function such as ceramide, glycosphingolipids, fatty acids, and lysophospholipids. Knowledge of the interfacial adsorption of Sphmase, precatalytic activation, initiation of effective catalysis, and the corresponding kinetic parameters is necessary for studying the level at which different lipids modulate the activity. We dissected some kinetic steps and determined the rate constants for degradation of Sphm, under controlled intermolecular organization, by Sphmase. Six models, adapted to two dimensions, were used to elucidate possible mechanisms for the interfacial activation of Sphmase during the lag time. The models consider enzyme binding to the substrate monolayer and a subsequent, essentially irreversible interfacial activation; this is supported experimentally by monolayer transfer experiments. Some mechanisms involve enzyme-substrate binding and associated states of the enzyme in the bulk subphase or at the interface, prior to complete activation. The activity of Sphmase is consistent with kinetics involving enzyme partitioning into the interface followed by substrate association, and by a process that proceeds with bimolecular kinetic dependence on the interfacial Sphmase concentration, and a subsequent slow step of activation. A possible equilibrium between the apparent monomolecular and bimolecular activated states of the interfacial enzyme, coupled to a slow activation, constitute rate-limiting steps that can explain the existence of lag time and the achievement of a maximum constant rate of degradation of Sphm monolayers by Sphmase.—Fanani, M. L., and B. Maggio. Kinetic steps for the hydrolysis of sphingomyelin by *Bacillus cereus* sphingomyelinase in lipid monolayers. *J. Lipid Res.* 2000. 41: 1832–1840.

**Supplementary key words** ceramide • phosphatidylcholine interfacial catalysis • interfacial activation • phospholipase kinetics

It is well established that the activity of several phospholipases from different sources is markedly affected by both the long-range physical state and the fine intermolecular organization of the phospholipid on which they act (1–5). Phosphohydrolytic enzymes, now almost all implicated in

some sort of membrane-mediated signal transduction (6, 7), are a heterogeneous group of proteins (8–10). In spite of this, all activities studied to date revealed a profound dependence on the same, few generic physicochemical parameters related to the structural dynamics of the lipid interface, with the critical regulatory values varying specifically for each enzyme within a relatively narrow range (5, 11–16).

The phospholipases that have been best studied in terms of their structural features and their regulation by phospholipid organization are the secretory and venom phospholipases A<sub>2</sub> and bacterial phospholipases C (2, 3, 11, 17–20), whereas biophysical studies of the mammalian membrane or cytosolic phospholipases are few (12, 13). More recently, interest has also been directed to the degradative pathway that involves the activity of a neutral sphingomyelinase (Sphmase), which produces ceramide that can be triggered by several stimuli in a variety of cellular effects (6, 21).

On the basis of the different cross-sectional molecular areas of sphingomyelin (Sphm) and ceramide in lipid monolayers, we previously showed that the activity of *Bacillus cereus* Sphmase can be followed in real time, while the catalytic reaction is taking place, with the intermolecular organization of the lipid substrate precisely controlled and continuously known (15). The technique was also used to follow the activity of *Staphylococcus aureus* Sphmase

Abbreviations: Cer, ceramide (*N*-acylsphingosine); d, a dimensionality factor for unit adjustment ( $d = 1 \text{ cm}$ );  $[E_{IT}]$ , the total enzyme concentration in the interface;  $[E_T]$ , the total enzyme concentration in the system;  $K$ , the enzyme-substrate association constant;  $k_{act}$ , the intrinsic kinetic constant for activation;  $k_{cat}$ , the catalytic constant of the reaction;  $K_d$ , the equilibrium constant for the formation of enzyme dimers;  $K_p$ , the partition constant of the enzyme between the bulk solution and the interface;  $K_s$ , the equilibrium binding constant of the substrate to the active site of the enzyme present in the interface; PLA<sub>2</sub>, phospholipase A<sub>2</sub> (EC 3.1.1.4); PLC, phospholipase C (EC 3.1.4.3);  $[S]$ , the two-dimensional concentration of substrate in the interface; SDS-PAGE, sodium dodecyl sulfate-polyacrylamide gel electrophoresis; Sphm, brain sphingomyelin; dlPC, (didodecanoyl-*sn*-glycero-3-phosphocholine); Sphmase, sphingomyelinase, *Bacillus cereus* sphingomyelin phosphodiesterase (EC 3.1.4.12);  $\tau$ , the lag time period.

<sup>1</sup> To whom correspondence should be addressed.

(22). We first reported that there is a surface-regulated interfacial cross-communication between the Sphm and glycerophospholipid degradation pathways mediated by Sphmase and phospholipase A<sub>2</sub> that is modulated by the presence of substrates and products of both reactions, depending in turn on the lateral surface pressure of the lipid interface (15, 16). These studies allowed us to describe the presence of a lag-time period before the maximum activity of Sphmase against Sphm monolayers is reached (15). This period involves interfacial adsorption and any precatalytic steps of enzymatic activation before the enzymatic activity can reach a steady state, that is, a constant rate of substrate degradation (pseudo zero-order kinetics), which is subsequently followed by a gradual halting of product formation (1, 15, 17, 19). Also, we showed that the modulation of Sphmase by different lipids and products of the phosphohydrolytic reaction catalyzed by phospholipase A<sub>2</sub> (PLA<sub>2</sub>) takes place at different levels that affect independently the steady state rate of catalysis and the lag-time period (16). This suggested that the interfacial regulation of these lipids could act at the levels of surface adsorption, interfacial enzyme activation at a precatalytic stage, and/or on the rate of effective catalysis (16). However, this analysis could proceed no further because, unlike other phospholipases (especially PLA<sub>2</sub>) that have been more extensively studied (23–26), the interfacial steps and the corresponding kinetic parameters have not yet been characterized for the reaction catalyzed by Sphmase acting on the pure substrate, let alone in more complex interfaces containing nonsubstrate lipids. The objective of the present work was to study the kinetic steps and to determine the equilibrium rate constants for the two-dimensional interfacial catalysis mediated by Sphmase acting on Sphm monolayers, under well-controlled conditions of intermolecular organization. This is a necessary prior basis for subsequent studies of the level at which different lipids may modulate the activity of Sphmase.

## MATERIALS AND METHODS

### Chemicals

Sphm and dilauroylphosphatidylcholine (dLPC) were purchased from Avanti Polar Lipids (Alabaster, AL). *Bacillus cereus* Sphmase (lot 48H4058) was obtained from Sigma-Aldrich (St. Louis, MO). Solvents and chemicals were of the highest commercial purity available, NaCl was roasted at 400°C for 4 h. The absence of surface active impurities in the solvents and buffers was routinely checked as described (17).

### Determination of enzymatic activity

Lipid monolayers were spread from premixed solutions of the desired lipid in chloroform-methanol (17) over a subphase of 10 mM Tris-HCl, 125 mM NaCl, 3 mM MgCl<sub>2</sub>, pH 8 (18bis). The reaction was followed in real time after injecting a concentrated solution of the enzyme into the subphase under an Sphm film, with continuous stirring, in a compartment of a specially designed thermostatted circular trough with an automatic surface barostat and adjacent reservoir compartments previously described in detail (17) (Fig. 1A). The activity of Sphmase was measured continuously against monolayers of the pure substrate at

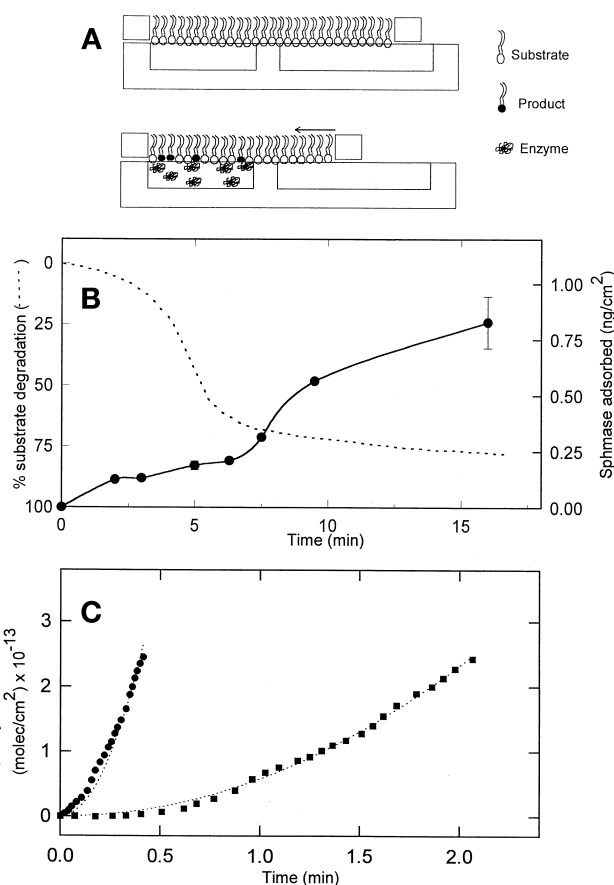


**Fig. 1.** Time course for hydrolysis of Sphm monolayers by Sphmase. (A) A simplified schematic of the trough and compartments used (see ref. 17). The percentage of substrate degradation (dotted line) and the amount of adsorbed enzyme at the interface (solid line) are shown in (B). (C) The initial portion of the curve for substrate degradation, when less than 10% of substrate has been degraded by 33 (solid circles) or 7 (solid squares) ng of enzyme per milliliter of subphase, added at time zero. As shown by the dotted lines fitting the points, there is a second-order dependence of the amount of substrate degraded with time. The reaction was carried out at  $25 \pm 1^\circ\text{C}$  and a constant surface pressure of 15 mN/m.

the air-buffer interface, at 25°C. A constant surface pressure of 15 mN/m is maintained for optimum activity by replenishment of pure Sphm from the reservoir compartment (15, 16); the enzyme activity is determined by recording of the reduction of the film area as a function of time caused by the progressive formation of ceramide (Cer) in the monolayer (15). The results represent average values from experiments performed at least in triplicate.

For some experiments Sphmase was labeled with <sup>125</sup>I to a suitable specific activity (approximately 1 μCi/μg protein) by stoichiometric iodination, using chloramine-T (27). When subjected to sodium dodecyl sulfate-polyacrylamide gel electrophoresis (SDS-PAGE), using either 7.5 or 15% polyacrylamide gels, *B. cereus* Sphmase showed only two components as visualized with Coomassie Brilliant Blue: more than 95% ran as a major band with a molecular weight of about 40,000 and the remaining component migrated with a molecular weight of about 24,000; it was previously reported that the latter value corresponded to that obtained by gel filtration and sedimentation equilibrium (28), while a molecular weight of 41,000 was obtained by SDS-PAGE (18). The molecular weight for Sphmase was taken as 24,000 in our

work. The amount of Sphmase adsorbed to the monolayer at different times after injection into the subphase was determined by measuring the radioactivity in a  $\gamma$  counter after collection of the film with hydrophobic paper (29). Complete collection of the monolayer containing the adsorbed enzyme was controlled by the decay of surface pressure to zero as described previously (17).

In the case of PLA<sub>2</sub>, the products of degradation are short-chain lysophospholipids and fatty acids that are quickly desorbed from the monolayer into the subphase (17), and the reaction in monolayers follows true zero order kinetics with respect to the surface concentration of substrate. This is different from the hydrolysis of Sphm by Sphmase, which produces Cer that remains in the film; in spite of this the existence of a pseudo-zero order kinetic period indicates an effective replenishment of Sphm and the maintenance of an operational substrate excess for a period of time independent of the proportions of product formed during this time. The slope of the linear portion (constant velocity in the pseudo-zero order region) of the curve of substrate degraded as a function of time after the lag time (when present) represents the maximum rate of activity at each enzyme concentration in the subphase (Fig. 1B). It should be emphasized that these pseudo-zero order rates are used only in the part of our analysis of the surface kinetics in which a classic Michaelis-Menten treatment of the data was applied (thus under conditions in which the activity proceeds independently of the mechanism that operated in the precatalytic interfacial activation of the enzyme); the rate of degradation during the pseudo-zero order reaction is linear starting from 0% degradation once the precatalytic activation steps have taken place (see Fig. 4). On the other hand, for the kinetic analysis of the precatalytic period we used only the initial portion of the reaction, during which less than 10% of the substrate was degraded (see Fig. 1B and C). We previously described the existence of lag time for the degradation of Sphm monolayers by Sphmase (15); the use of only the initial portion of the reaction for the kinetic analysis of the precatalytic period is validated because interfacial enzyme activation occurs that is independent of the presence of effective catalysis as shown in experiments with transferred monolayers (see Fig. 4). The presence of lag time in phosphohydrolytic reactions in monolayers and bilayer vesicles (3, 11, 17, 19, 20, 23–25) reveals the requirement for interfacial steps that must take place before a constant rate of substrate degradation can be reached. Although there are no theoretical reasons for preferences, the lag time in monolayer experiments is usually defined as that time necessary to reach a constant velocity and is taken by extrapolation of the linear portion of the curve for activity in Fig. 1B to the point on the time axis corresponding to zero substrate degradation (1, 15, 19, 20). However, in work done with phospholipases acting on unilamellar lipid vesicles (23–25) the lag time has frequently been defined in a different operational (although conceptually similar) manner as the time taken by the reaction to reach half of the maximum rate of activity (constant velocity). In this work, the latter definition for the monolayer lag time was adopted mostly because it simplifies the mathematical treatment used in the kinetic models.

### Kinetic models

Several kinetic models were proposed to describe the complex reaction catalyzed by various types of secretory phospholipases A<sub>2</sub> (PLA<sub>2</sub>). Most of these models attempted mainly to elucidate possible mechanisms of interfacial activation of the enzymes during the lag-time period that occurs before catalytic formation of product reaches a steady state (23, 24, 30).

To explore the kinetic steps for the degradation of Sphm monolayers by Sphmase we adapted to two-dimensional kinetics three models previously used to study the degradation of bilayer

vesicles by secretory PLA<sub>2</sub> (23, 30, 31). In these models it is assumed that the enzyme binds to the surface formed by the organized substrate phospholipid by a rapid equilibrium and subsequently undergoes an essentially irreversible interfacial activation. Three additional models were developed by introducing a first step represented by an unspecific partition of the enzyme in the interface and considering the association of Sphmase to the substrate Sphm as a subsequent step to the interfacial partition, followed by a step showing a bimolecular dependence with the enzyme concentration (see below) prior to activation. For the precatalytic steps of Sphmase the experimental data were analyzed using the initial portion of the reaction under conditions in which less than 10% of the substrate was degraded (see Fig. 1B and C). The adsorption of Sphmase to the monolayer is operationally irreversible and the film containing the active enzyme can be transferred and washed repetitively over enzyme-free compartments with negligible desorption. After these cycles, Sphmase remains irreversibly activated and the two-dimensional reaction begins without lag time, with catalysis proceeding under steady state conditions of constant velocity (see Fig. 4) (16). This demonstrates directly that, similar to PLA<sub>2</sub> and phospholipase C (PLC) (19, 32), precatalytic activation steps for the Sphmase already at the interface can occur dissociated from those of effective hydrolytic catalysis under conditions in which the latter is not taking place.

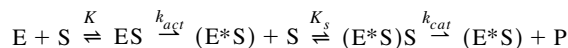
All the models used in this work show that the amount of product formed as a function of time in the initial part of the reaction (less than 10% substrate degraded) (Fig. 1C) can be fitted by a second-order equation of the type

$$[P]_{(t)} = A_i t^2$$

Some of the kinetic mechanisms investigated below involve the formation of associated states of the enzyme in the bulk subphase or at the interface. The experimental dependence of the second-order coefficient and of the lag time on the two-dimensional concentration of enzyme in the interface (Figs. 5 and 6B) are compatible with a bimolecular process related to enzyme-enzyme interaction. For this reason, and by analogy to mechanisms proposed for some phosphohydrolytic reaction mediated by different secretory PLA<sub>2</sub> (23, 24), we simulate operationally (on kinetic but not necessarily on molecular terms) these steps as enzyme “dimerization.” As far as we know, the interfacial kinetics of *B. cereus* Sphmase against lipid monolayers or bilayers, in the absence of detergents, has not been studied in detail. The estimation of its molecular weight by gel filtration and sedimentation equilibrium indicates that *B. cereus* Sphmase does not undergo dimerization in solution (28), a condition that may also be reached from the kinetic analysis given below. On the other hand, it should also be noticed (see Materials and Methods) that when dispersed in the presence of the detergent amphiphath SDS the protein undergoes dimerization (18). We emphasize that the type of kinetics exhibited by Sphmase in monolayers could also be accounted for by a more complex surface process that the enzyme might mediate, leading to a phenomenologically apparent bimolecular cooperativity (i.e., interfacial cooperative changes of the whole protein or subdomain conformation, substrate clustering at the interface mediated bimolecularly by the enzyme, thermodynamically coupled synergistic formation of product by enzyme molecules not necessarily in direct contact in the interface but simultaneously needed to achieve catalysis through structural-dynamic changes of the lipid-protein substrate organization). Some of these phenomena have been mentioned (2, 14, 33), as well as the visualization of interfacial enzyme clustering (34) of unknown cooperativity for catalysis, as possible factors participating in the regulation of lipolysis.

The kinetic models involve the following steps.

**Model I.** It is assumed that there is a penetration of the enzyme in the lipid interface while binding to the substrate, followed by a slow activation process before reaching maximum catalytic capacity. This model also assumes that the amount of activated enzyme is negligible compared with the total.



$$[P]_{(t)} = \frac{k_{cat}k_{act}K_sK[S]^2[E_T]d}{2(1+K[S])(1+K_s[S])} t^2 \quad Eq. 1)$$

$$\tau = \frac{1+K[S]}{2k_{act}K[S]} \quad Eq. 2)$$

**Model II.** Model II assumes a rapid equilibrium between a monomeric and a dimeric state of the enzyme in solution, with the equilibrium displaced in favor of the monomer; only the dimer form can bind to the interface and undergoes a slow activation. It is also assumed that the amount of enzyme adsorbed to the interface is much smaller compared with the soluble form.

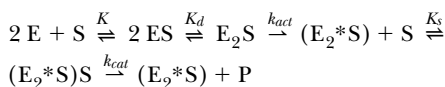


$$(E_2^*S)S \xrightarrow{k_{cat}} (E_2^*S) + P$$

$$[P]_{(t)} = \frac{k_{cat}k_{act}K_dK_sK[S]^2([E_T]d)^2}{2(1+K_s[S])} t^2 \quad Eq. 3)$$

$$\tau = \frac{1}{2k_{act}K_dK[S]([E_T]d)} \quad Eq. 4)$$

**Model III.** Model III assumes a dimerization step after the enzyme associates to the substrate in the interface, and that only the dimer form is active. Again it is assumed that the amount of activated enzyme is small.

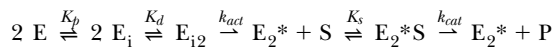


$$(E_2^*S)S \xrightarrow{k_{cat}} (E_2^*S) + P$$

$$[P]_{(t)} = \frac{k_{cat}k_{act}K_dK_sK^2[S]^2([E_T]d)^2}{2(1+K[S])^2(1+K_s[S])} t^2 \quad Eq. 5)$$

$$\tau = \frac{(1+K[S])^2}{2k_{act}K_dK^2[S]([E_T]d)} \quad Eq. 6)$$

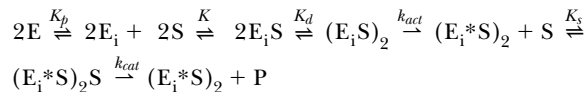
**Model IV.** Like model III, model IV proposes a dimerization of the enzyme associated with the lipid interface but preceded by a step involving nonspecific partitioning of the enzyme to the interface without initial substrate binding. As in the other models, it is assumed that the amount of activated enzyme is small.



$$[P]_{(t)} = \frac{k_{cat}k_{act}K_dK_p^2K_s[S]^2([E_T]d)^2}{2(1+K_p)^2(1+K_s[S])} t^2 \quad Eq. 7)$$

$$\tau = \frac{(1+K_p)^2}{2k_{act}K_dK_p^2[S]([E_T]d)} \quad Eq. 8)$$

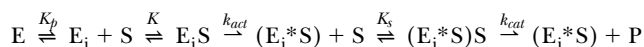
**Model V.** The proportion of enzyme initially partitioning in the lipid interface ( $K_p$ ) was separately obtained experimentally and not included in equations 9 and 10. After the partition step the model involves association of the enzyme with the substrate and subsequent dimerization before activation. In this model the amount of activated enzyme is assumed to be much smaller than the total amount of enzyme at the interface.



$$[P]_{(t)} = \frac{k_{cat}k_{act}K_dK_sK^2[S]^2[E_{iT}]^2}{2(1+K[S])^2(1+K_s[S])} t^2 \quad Eq. 9)$$

$$\tau = \frac{(1+K[S])^2}{2k_{act}K_dK^2[S][E_{iT}]} \quad Eq. 10)$$

**Model VI.** As in model V, the proportion of enzyme partitioning initially to the interface ( $K_p$ ) was separately obtained experimentally and not included in equations 11 and 12. After the partition step the model assumes no dimerization and involves association of the enzyme to the substrate prior to activation, similar to model I. Again, the model assumes that the amount of activated enzyme is smaller than the total amount of enzyme in the interface.



$$[P]_{(t)} = \frac{k_{cat}k_{act}K_sK[S]^2[E_{iT}]}{2(1+K[S])(1+K_s[S])} t^2 \quad Eq. 11)$$

$$\tau = \frac{(1+K[S])}{2k_{act}K[S]} \quad Eq. 12)$$

**Combination model V–VI.** Combination model V–VI considers the possibility of having two populations of enzyme molecules acting simultaneously but independently as monomers and dimers in the interface. It results from a linear combination of equations 9 and 11.

$$[P]_{(t)} = (A_V + A_{VI}) t^2 \quad Eq. 13)$$

$$[P]_{(t)} = \left[ \frac{k_{cat}k_{act}K_sK[S]^2[E_{iT}]}{2(1+K[S])(1+K_s[S])} \left( 1 + \frac{K_dK[E_{iT}]}{(1+K[S])} \right) \right] t^2 \quad Eq. 14)$$

In all the equations,  $K$  is the enzyme-substrate association constant,  $K_s$  is the equilibrium binding constant of the substrate to the active site of the enzyme present in the interface (being  $K_s = K_M^{-1}$ , where  $K_M$  is the Michaelis-Menten constant).  $K_d$  is the equilibrium constant for the formation of enzyme dimers.  $K_p$  is the partition constant of the enzyme between the bulk solution and the interface.  $k_{act}$  is the intrinsic kinetic constant for activation.  $k_{cat}$  is the catalytic constant of the reaction.  $d$  is a dimensionality factor for unit adjustment ( $d = 1$  cm).  $[E_T]$  is the total enzyme concentration in the system.  $[E_{iT}]$  is the total enzyme concentration in the interface.  $[S]$  is the two-dimensional concentration of substrate in the interface.  $\tau$  is the lag time as defined above.

## RESULTS AND DISCUSSION

### Interfacial adsorption

The hydrolytic reaction of Sphm by Sphmase in monolayers develops as a function of time as shown in Fig. 1B. During the latency period the amount of Sphmase adsorbed to the interface formed initially by the pure substrate slowly increases up to a plateau that begins at the end of the lag time and remains constant through the pseudo-zero order region of constant velocity. During this time the interface becomes progressively enriched in Cer and, when the substrate has been degraded by about 70–80%, the re-

action velocity decreases gradually to zero while a further adsorption of the enzyme takes place. This result becomes important when considering the kinetic models because it experimentally shows that the partitioning of the enzyme to the interface is not impaired by the formation of product.

**Figure 2** shows the amount of enzyme adsorbed to the interface ( $E_{iT}$ ) as a function of the total concentration of enzyme in the subphase ( $E_T$ ). The association of the enzyme to the interface saturates when the concentration in the subphase is about  $310 (\pm 40) \times 10^9$  molecules  $\text{cm}^{-3}$ . From these experimental data the (interface/subphase) partition constant ( $K_p$ ) can be obtained. As in previous studies (35), to account for compatible units we used a thickness of the interface that corresponds to one enzyme diameter, assuming a spherical symmetry for the protein molecule; changes in the interfacial thickness by 0.5- to 2-fold do not introduce variations on the order of magnitude of the calculated  $K_p$ . The value obtained for  $K_p$  ( $7 \times 10^4$ ) indicates the high tendency of the enzyme to associate with the lipid interface and is of the order found for other proteins that can become associated with lipid monolayers (35).

### Pseudo-zero order catalytic reaction

After the lag time, the reaction proceeds with constant velocity ( $V_0$ ) during the period corresponding to pseudo-

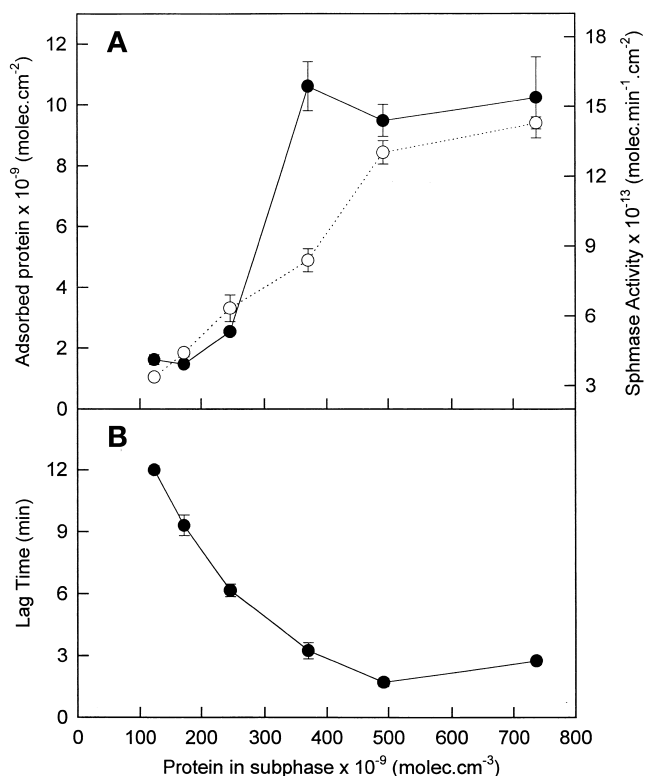


**Fig. 2.** Interfacial adsorption and activity of  $^{125}\text{I}$ -labeled Sphmase at various subphase concentrations. The dependence of enzyme adsorption (A, solid circles), the rate of Sphmase activity (A, open circles), and the lag time (B) on the subphase enzyme concentration is shown. The three measurements were obtained simultaneously in each reaction curve. The results represent average values  $\pm$  SEM; where no error bars can be seen these are within the size of the point.

zero order kinetics. Without taking into account the period of lag time (at the end of which the interfacial activation of the enzyme is completed) the dependence of  $V_0$  with the two-dimensional concentration of substrate can be used to analyze the kinetics of the reaction catalyzed by the active enzyme according to a classic Michaelis-Menten treatment, independent of whichever mechanism operated for enzyme activation. The substrate Sphm is “diluted” at a constant surface pressure in the monolayer by mixing it in different proportions with dlPC. We previously reported that dlPC does not affect Sphmase activity (15, 16) and control experiments showed that this lipid mixes ideally with Sphm and does not affect its molecular parameters at all proportions in the monolayer (this was concluded on the basis of no deviations found of mean molecular areas and mean surface potential/molecule as a function of the mole fraction of the components, at different surface pressure). Under these conditions, only the active enzyme population associated with the interface was considered for the kinetic analysis:

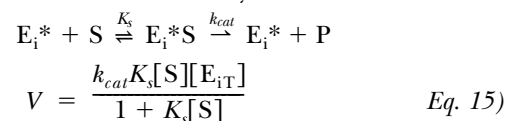


**Figure 3** shows the variation of  $V_0$ , normalized by the actual amount of enzyme adsorbed to the interface at each point of substrate concentration, as a function of the two-dimensional concentration of Sphm. Inhibition of activity is observed at values of  $[S]$  above  $6 \times 10^{13}$  molecules/ $\text{cm}^2$  (which corresponds to a monolayer with 50% Sphm and

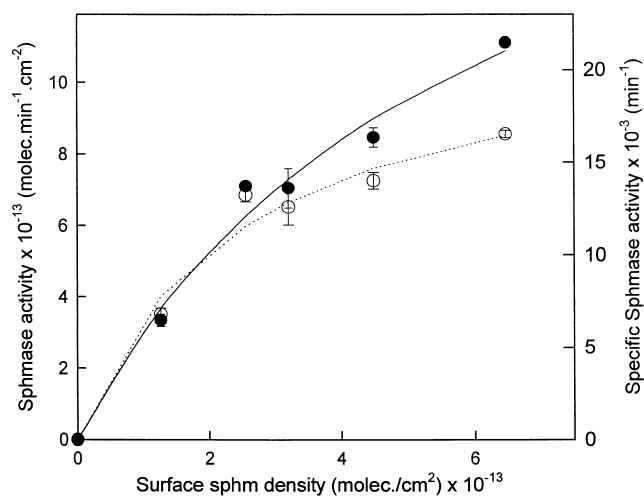


**Fig. 3.** Interfacial substrate dependence of Sphmase activity. The rate of activity (solid circles) and the specific activity (open circles) of  $^{125}\text{I}$ -labeled Sphmase acting against films with various surface concentrations of substrate are shown. Above the maximum value of Sphm concentration indicated on the abscissa, a gradual inhibition of the activity is observed. The reaction was carried out at a constant surface pressure of 15 mN/m. The surface dilution of Sphm is achieved by spreading mixed monolayers from premixed solvent solutions of Sphm and dlPC, as neutral diluent (see Materials and Methods), in the desired proportions. The results represent average values  $\pm$  SEM; where no error bars can be seen these are within the size of the point.

TABLE 1. Kinetic parameters for the hydrolysis of sphingomyelin monolayers by sphingomyelinase<sup>a</sup>

From	Parameters	Units	Value
Interfacial adsorption	$K_p$		$7 \times 10^4$
Pseudo-zero order catalytic reaction	$K_s$	$10^{-13} \text{ cm}^2 \text{ molecule}^{-1}$	0.4
	$k_{cat}$	$\text{sec}^{-1}$	$4 \times 10^2$
Activation steps (model V)	$k_{cat}k_{act}$	$\text{sec}^{-2}$	1
	$k_{act}K_d$	$10^{-13} \text{ cm}^2 \text{ molecule}^{-1} \text{ sec}^{-1}$	$5 \times 10^2$
	$K_d$	$10^{-13} \text{ cm}^2 \text{ molecule}^{-1}$	$1 \times 10^4$
	$K_s$	$10^{-13} \text{ cm}^2 \text{ molecule}^{-1}$	Not unequivocally determined, greater than 1
	$K$	$10^{-13} \text{ cm}^2 \text{ molecule}^{-1}$	Not unequivocally determined, greater than 1
	$k_{cat}^b$	$\text{sec}^{-1}$	$2 \times 10^2$
	$k_{act}^b$	$\text{sec}^{-1}$	$5 \times 10^{-3}$

<sup>a</sup> The results were calculated from the different approaches stated in column 1.

<sup>b</sup> Calculated from activation step data.

50% dlPC). The analysis of the hyperbolic curve shows values of  $K_s$  and  $k_{cat}$  of  $0.4 \times 10^{-13} \text{ cm}^2/\text{molecule}$  and  $4 \times 10^2 \text{ sec}^{-1}$ , respectively (Table 1).

### Activation steps

**Qualitative analysis.** Figure 4 shows that this enzyme, similar to porcine pancreas PLA<sub>2</sub> and *B. cereus* PLC (19, 32), does not desorb from the monolayer interface after successive film transfer and rinsing over enzyme-free subphases and does not exhibit lag time when the surface pressure is decreased below the cutoff point for activity. This indicates that both the enzyme partition to the interface and the interfacial activation steps have occurred in an essentially irreversible manner. On these bases all the kinetic models proposed in this work consider a practically irreversible activation step preceded by several rapid equilibria.

To differentiate the existence of an operational step (that is bimolecularly dependent with respect to the enzyme concentration) prior to activation, and whether this takes place in the subphase solution or at the interface, the initial phase of the reaction was analyzed. In this period the degradation of substrate is below 10% and the reaction clearly shows a second-order dependence with time as exemplified in Fig. 1C for two different concentrations of enzyme,  $[E_T]$ , in the subphase. The dependence of the second-order coefficient A with the total enzyme concentration  $[E_T]$  (not shown) and with the interfacial concentration of enzyme  $[E_{IT}]$  (Fig. 5) for the kinetic models proposed was analyzed. The experimental values indicate a quadratic dependence of the second-order coefficient with the total and with the interfacial enzyme concentration, suggesting the existence of a bimolecular step referred to the enzyme that could, in principle, be accounted for by models II, III, and V and by combination model V–VI. The lag-time period, as defined for the activity of phospholipases A<sub>2</sub> against bilayer vesicles, is the time taken for the reaction to reach half the maximum velocity (half the constant velocity  $V_0$ ). In Materials and Methods the equations representing the lag time for the different models are given. The dependence of the lag time ( $\tau$ ) on the two

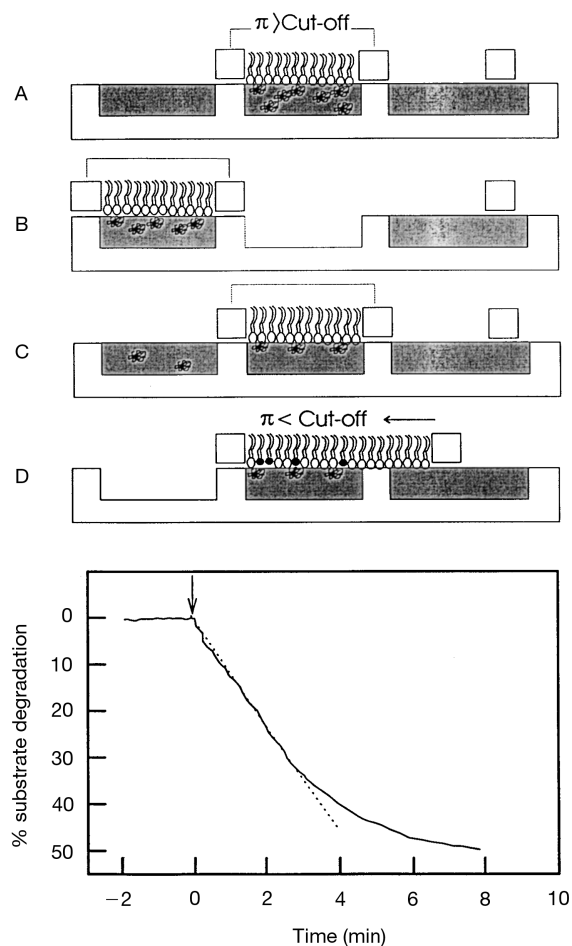


**Fig. 4.** Film transfer experiment. Shown is the actual time course of one representative experiment. The Sphm monolayer was exposed to a subphase containing enzyme (20 ng/ml) incubated with enzyme at a surface pressure of 25 mN/m, which is above its cutoff point (15) for activity (A). The film was subsequently transferred onto an enzyme-free subphase at a constant surface pressure of 25 mN/m (B), kept there for 10 min, and transferred again over a fresh subphase without enzyme (C). The film was then quickly (within 30 sec) relaxed to 15 mN/m (D, arrow). As shown in the plot in the lower part the reaction starts without lag time. The arrow shows the time when the film is relaxed to 15 mN/m.

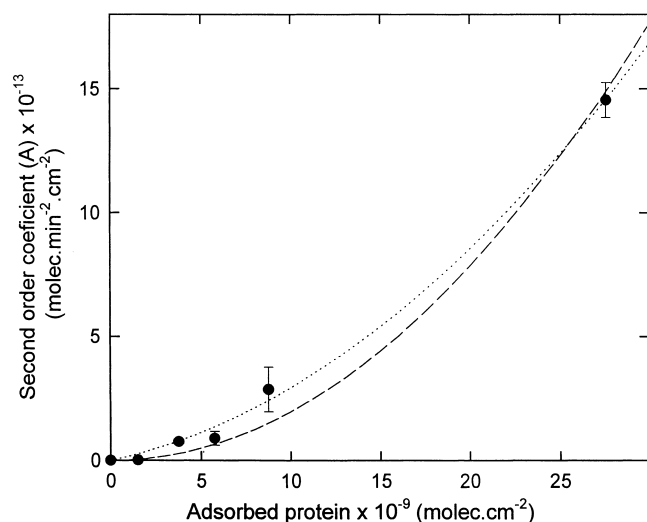


**Fig. 5.** Dependence of the second-order coefficient  $A$  on the adsorbed protein surface concentration. The curve could be fitted by model II, III, or V (see Materials and Methods) as a quadratic expression (dashed curve); a better fit includes a linear term as taken into account by the combination of models V and VI (dotted curve). The results represent average values  $\pm$  SEM; where no error bars can be seen these are within the size of the point.

dimensional concentration of substrate and on the enzyme concentration in the interface (**Fig. 6**) indicates that only models III and V can adequately fit the experimental values.

Also, the dependence of the second-order coefficient  $A$  on the two-dimensional concentration of Sphm  $[S]$  (**Fig. 7**) clearly shows that only models III and V (and combination model V–VI, only if the contribution of model VI is small, see below) can fit the experimental data.

**Quantitative analysis.** As discussed above, models III and V can qualitatively describe the experimental results. However, several of the kinetic constants obtained after fitting the data with model III were inconsistent among them or could not reach meaningful convergence. To adjust this problem, in models IV, V, and VI the adsorption of the enzyme to the interface was considered as a partition equilibrium between the subphase and the interfacial milieu as an initial step independent of a specific association with the substrate, with the latter event occurring after the partition has taken place. Because the partition constant  $K_p$  was experimentally determined in our work, model V could be analyzed from the step in which the enzyme is already in the interface onward; this eliminated the inconsistencies and the fitting algorithms could proceed to successful convergence. The complete fitting analysis provides the data shown in Table 1.

The data in Table 1 result from the combined analysis of the dependence of the second-order coefficient  $A$  (**Fig. 7**) and the lag time (**Fig. 6**) with  $[S]$  and with  $[E_{IT}]$  (**Figs. 5** and **6**). As shown in **Fig. 5**, a better fitting of the experimental data is obtained if a linear term in  $[E_{IT}]$  is introduced in equation 9. This essentially represents the linear combination of model V with model VI (see equa-

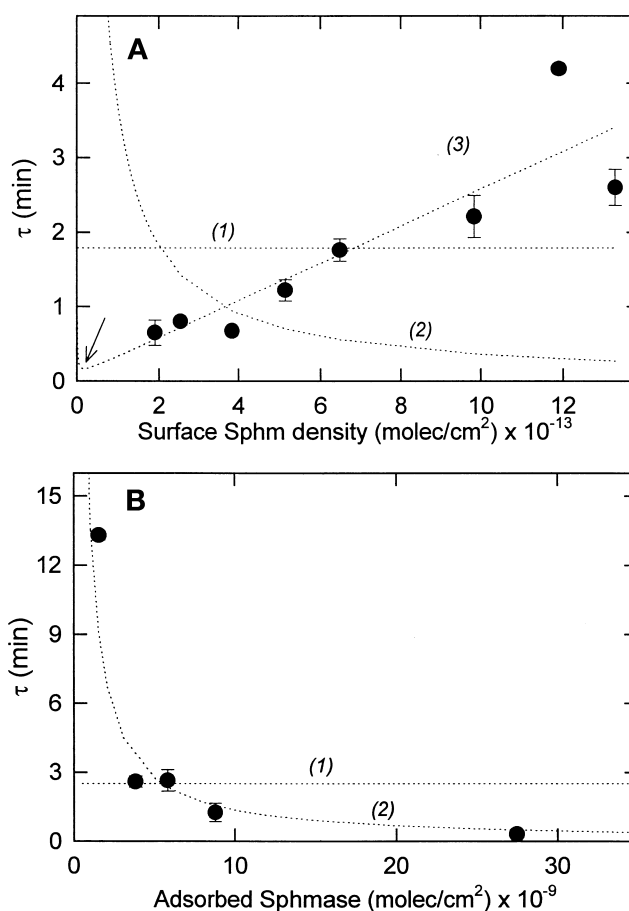


**Fig. 6.** Dependence of the lag time  $\tau$  with the surface concentration of substrate and enzyme. (A) The experimental dependence of  $\tau$  on the Sphm surface concentration (diluted with dIPC as in **Fig. 3**). Dotted curves represent the best fitting by model I or VI (1), II or IV (2), and III or V (3). Curve (3) shows a well-defined minimum (arrow) at a substrate concentration of  $0.15 \times 10^{13}$  (molecules  $\text{cm}^{-2}$ ). (B) The experimental dependence of  $\tau$  on the adsorbed  $^{125}\text{I}$ -labeled Sphmase surface concentration. Dotted curves represent the best fitting by model I or VI (1), and by model II, III, IV, or V (2). The results represent average values  $\pm$  SEM; where no error bars can be seen these are within the size of the point.

tions 13 and 14) and the mathematical fit suggests the presence of two enzyme populations in the interface, one acting in the reaction with a monomolecular and the other with a bimolecular dependence on the Sphmase concentration at the interface. However, from the combination of both models the value of  $K_d$  is  $1 \times 10^4$  (in units of  $10^{-13} \text{ cm}^2 \text{ molecule}^{-1}$ ) and this value indicates that only about 0.07% of the interfacial enzyme should be acting monomolecularly. In practical terms, therefore, model V offers the more plausible kinetic representation of the experimental data.

From model V, the equilibrium binding constant of the substrate to the active site of the enzyme present in the interface,  $K_s$ , and the association enzyme-substrate constant  $K$  are not unequivocally determined as single figures and several values can give equally good fits. However, only when these constants are greater than 1 do the figures for all the rest of the kinetic parameters remain independent

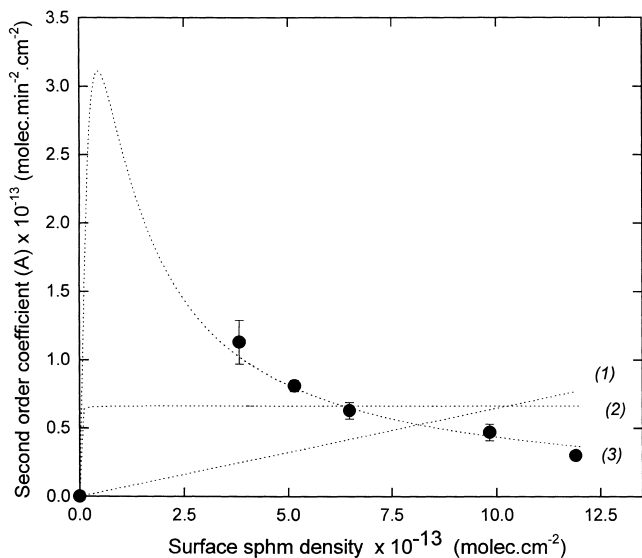


**Fig. 7.** Dependence of the second-order coefficient  $A$  on the substrate surface concentration. The dotted lines represent the best fit of the experimental data by model II or IV (curve 1), I or VI (curve 2), and III or V (curve 3). The results represent average values  $\pm$  SEM; where no error bars can be seen these are within the size of the point.

of the values of  $K_s$  and  $K$ . In this manner these constants effectively describe equilibrium situations, with enzyme activation being the rate-limiting step for the reaction. When the values for  $K_s$  and  $K$  are less than 1, to adequately fit the experimental data the values of  $K_d$  and  $k_{cat}k_{act}$  should increase exponentially as  $K_s$  and  $K$  tend to zero. This dependence indicates that when the association steps described by the latter constants ( $K$  and  $K_s$ ) become slow these processes become the rate-limiting steps for the interfacial degradation of Sphm and all subsequent steps become dependent on the rate of their occurrence. On the other hand, classic Michaelis-Menten analysis that is performed using the data obtained under conditions in which the reaction is proceeding in the constant velocity region (and thus independently of the mechanisms for activation) gives a defined value for  $K_s$  of 0.4. It is interesting that this value is in the range discussed above, which suggests that the initial processes involved in the interfacial association of the enzyme could act as key regulatory steps for the reaction. The value of  $k_{cat}$  calculated from the classic kinetic analysis is  $4 \times 10^2$ , which is of the same order and totally in keeping (only twice the figure and the same order of magnitude) with the value for this constant obtained from the fitting of the data by model V, with values for  $K_s$  and  $K$  above 1 (Table 1); this supports the idea that enzyme activation and formation of product are rather slow and irreversible steps.

In conclusion, the kinetics of the phosphohydrolytic reaction catalyzed by Sphmase in monolayers of pure Sphm is consistent with a mechanism involving an initial enzyme partition into the interface, a subsequent step that can operationally be simulated as a surface process depending bimolecularly on the interfacial concentration of enzyme

(which would be kinetically indistinguishable from a dimerization process of the enzyme bound to the substrate; see Materials and Methods), and a subsequent step of activation. About 99.93% of the enzyme bound to the interface is probably acting bimolecularly [ $K_d = 1 \times 10^4$  ( $10^{-13}$  cm $^2$  molecule $^{-1}$ )]. The kinetics of activation is slow compared with the rate of catalysis ( $k_{act} = 3 \times 10^{-3}$  and  $k_{cat} = 4 \times 10^2$ ). This indicates that the establishment of an equilibrium between apparent monomolecular and bimolecular activated states of the enzyme in the interface, coupled to a slow activation process, appears to constitute the rate-limiting steps that can explain the existence of the lag time in the reaction catalyzed by *B. cereus* Sphmase in Sphm monolayers. ■

This work was supported in part by SECyT-UNC, CONICET, CONICOR, and FONCyT, Argentina. M.L.F. is a Fellow and B.M. is Principal Investigator of CONICET, Argentina.

Manuscript received 15 February 2000 and in revised form 12 June 2000.

## REFERENCES

1. Ransac, S., H. Moreau, C. Riviere, and R. Verger. 1991. Monolayer techniques for studying phospholipase kinetics. *Methods Enzymol.* **197**: 49–65.
2. Honger, T., K. Jorgensen, D. Stokes, R. L. Biltonen, and O. G. Mouritsen. 1997. Phospholipase  $A_2$  activity and physical properties of lipid-bilayer substrates. *Methods Enzymol.* **286**: 168–191.
3. Jain, M. K., J. Rogers, D. V. Jahagirdar, J. F. Marecek, and F. Ramirez. 1986. Kinetics of interfacial catalysis by phospholipase  $A_2$  in intravesicle scooting mode, and heterofusion of anionic and zwitterionic vesicles. *Biochim. Biophys. Acta.* **860**: 435–447.
4. Ruiz-Arguello, M. B., F. M. Goñi, and A. Alonso. 1998. Vesicle membrane fusion induced by the concerted activities of Sphmase and phospholipase C. *J. Biol. Chem.* **273**: 22977–22982.
5. Maggio, B. 1996. Control by ganglioside GD1a of phospholipase  $A_2$  activity through modulation of the lamellar-hexagonal (HII) phase transition. *Mol. Membr. Biol.* **13**: 109–112.
6. Hannun, Y. A., and R. M. Bell. 1989. Functions of sphingolipids and sphingolipid breakdown products in cellular regulation. *Science.* **243**: 500–507.
7. Exton, J. H. 1990. Signaling through phosphatidylcholine breakdown. *J. Biol. Chem.* **265**: 1–4.
8. Gatt, S. 1999. Studies of sphingomyelin and sphingomyelinases. *Chem. Phys. Lipids.* **102**: 45–53.
9. Heinz, D. W., L. Essen, and R. L. Williams. 1998. Structural and mechanistic comparison of prokaryotic and eukaryotic phosphoinositide-specific phospholipases C. *J. Mol. Biol.* **275**: 635–650.
10. Roberts, M. F. 1996. Phospholipases: structural and functional motifs for working at an interface. *FASEB J.* **10**: 1159–1172.
11. Volwerk, J. J., E. Filthuth, O. H. Griffith, and M. K. Jain. 1994. Phosphatidylinositol-specific phospholipase C from *Bacillus cereus* at the lipid-water interface: interfacial binding, catalysis, and activation. *Biochemistry.* **33**: 3464–3474.
12. Bouguaslavsky, V., M. Rebecchi, A. J. Morris, D. Y. Jhon, S. G. Rhee, and S. McLaughlin. 1994. Effect of monolayer surface pressure on the activities of phosphoinositides—specific phospholipase C- $\beta$ 1,  $\gamma$ 1 and  $\delta$ 1. *Biochemistry.* **33**: 3032–3037.
13. James, S. R., A. Paterson, T. K. Harden, R. A. Demel, and C. P. Downes. 1997. Dependence of the activity of phospholipase C $\beta$  on surface pressure and surface composition in phospholipid monolayers and its implications for their regulation. *Biochemistry.* **36**: 848–855.
14. Muderhwa, J. M., and H. L. Brockman. 1992. Lateral lipid distribution is a major regulator of lipase activity: implications for lipid-mediated signal transduction. *J. Biol. Chem.* **267**: 24184–24192.
15. Fanani, M. L., and B. Maggio. 1997. Mutual modulation of sphingomyelinase and phospholipase  $A_2$  activities against mixed lipid



- monolayers by their lipid intermediates and glycosphingolipids. *Mol. Membr. Biol.* **14**: 25–29.
16. Fanani, M. L., and B. Maggio. 1998. Surface pressure-dependent cross-modulation of sphingomyelinase and phospholipase A<sub>2</sub> in monolayers. *Lipids*. **33**: 1079–1087.
  17. Maggio, B., I. D. Bianco, G. G. Montich, G. D. Fidelio, and R. K. Yu. 1994. Regulation by gangliosides and sulfatides of phospholipase A<sub>2</sub> activity against dipalmitoyl- and dilauroylphosphatidylcholine in small unilamellar bilayer vesicles and mixed monolayers. *Biochim. Biophys. Acta*. **1190**: 137–148.
  18. Tomita, M., R. Taguchi, and H. Ikezawa. 1982. Molecular properties and kinetic studies on sphingomyelinase of *Bacillus cereus*. *Biochim. Biophys. Acta*. **704**: 90–99.
  19. Bianco, I. D., G. D. Fidelio, R. K. Yu, and B. Maggio. 1991. Degradation of dilauroylphosphatidylcholine by phospholipase A<sub>2</sub> in monolayers containing glycosphingolipids. *Biochemistry*. **30**: 1709–1714.
  20. Bianco, I. D., G. D. Fidelio, and B. Maggio. 1990. Effect of sulfate and gangliosides on phospholipase C and phospholipase A<sub>2</sub> activities. A monolayer study. *Biochim. Biophys. Acta*. **1026**: 179–185.
  21. Kolesnik, R. N. 1991. Sphingomyelin and derivatives as cellular signals. *Prog. Lipid Res.* **30**: 1–38.
  22. Jungner, M., H. Ohvo, and P. Slotte. 1997. Interfacial regulation of bacterial sphingomyelinase activity. *Biochim. Biophys. Acta*. **1344**: 230–240.
  23. Romero, G., K. Thompson, and R. L. Biltonen. 1987. The activation of porcine pancreatic phospholipase A<sub>2</sub> by dipalmitoylphosphatidylcholine large unilamellar vesicles. Analysis of the state of aggregation of the activated enzyme. *J. Biol. Chem.* **262**: 13476–13482.
  24. Bell, J. D., and R. L. Biltonen. 1992. Molecular details of the activation of soluble phospholipase A<sub>2</sub> on lipid bilayers. *J. Biol. Chem.* **267**: 11046–11056.
  25. Ferrato, F., F. Carriere, L. Sarda, and R. Verger. 1997. A critical re-evaluation of the phenomenon of interfacial activation. *Methods Enzymol.* **286**: 327–347.
  26. Burack, W. R., M. E. Gadd, and R. L. Biltonen. 1995. Modulation of phospholipase A<sub>2</sub>: identification of an inactive membrane-bound state. *Biochemistry*. **34**: 14819–14828.
  27. Roth, J. 1975. Methods for assessing immunologic and biologic properties of iodinated peptide hormones. *Methods Enzymol.* **37**: 223–233.
  28. Ikezawa, H., M. Mori, T. Ohyabu, and R. Taguchi. 1978. Studies on sphingomyelinase of *Bacillus cereus*. I. Purification and properties. *Biochim. Biophys. Acta*. **528**: 247–256.
  29. Momsen, W. E., and H. L. Brockman. 1997. Recovery of monomolecular films in studies of lipolysis. *Methods Enzymol.* **286**: 292–305.
  30. Verger, R., M. C. E. Mieras, and G. H. de Haas. 1973. Action of phospholipase A at interface. *J. Biol. Chem.* **248**: 4023–4034.
  31. Wells, M. A. 1971. Evidence that the phospholipase A<sub>2</sub> of *Crotalus adamanteus* venom are dimers. *Biochemistry*. **10**: 4074–4078.
  32. Daniele, J. J., B. Maggio I. D. Bianco, F. M. Goñi, A. Alonso, and G. D. Fidelio. 1996. Inhibition by gangliosides of *Bacillus cereus* phospholipase C activity against monolayers, micelles and bilayer vesicles. *Eur. J. Biochem.* **239**: 105–110.
  33. Holopainen, J. M., M. Subramanian, and P. K. J. Kinnunen. 1998. sphingomyelinase induces lipid microdomain formation in a fluid phosphatidylcholine/sphingomyelin membrane. *Biochemistry*. **37**: 17562–17570.
  34. Grainger, D. W., A. Reichert, H. Ringsdorf, and C. Salesse. 1990. Hydrolytic action of phospholipase A<sub>2</sub> in monolayers in the phase transition region: direct observation of enzyme domain formation using fluorescence microscopy. *Biochim. Biophys. Acta*. **1023**: 365–379.
  35. Fidelio, G. D., B. Maggio, and F. A. Cumar. 1986. Stability and penetration of soluble and membrane proteins in interface. *An. Asoc. Quím. Argent.* **74**: 801–813.